CHIN. PHYS. LETT. Vol. 36, No. 11 (2019) 117302

Fe-Doped All-Boron Fullerene B_{40} with Tunable Electronic and Magnetic Properties as Single Molecular Devices *

An-Zhi Xie(谢安治), Tian-Zhen Wen(文天珍), Ji-Ling Li(李继玲)**
School of Materials Science & Engineering, Sun Yat-sen University, Guangzhou 510275

(Received 24 July 2019)

Systematic theoretical calculations are performed to investigate the dopant effect of Fe on stability, electronic and magnetic properties of the newly synthesized all-boron fullerene B_{40}. The results reveal that as a typical ferromagnetic element, Fe atoms can either be chemically externally adsorbed on, or internally encapsulated in the cage of B_{40}, with the binding energies ranging from 3.07 to 5.31 eV/atom. By introducing the dopant states from the doped Fe atom, the energy gaps of the Fe-doped B_{40}-based metallofullerenes are decreased. Our spin-polarized calculations indicate that Fe-doped metallofullerenes have attractive magnetic properties: with alternative binary magnetic moments between $4.00\mu_B$ and $2.00\mu_B$, depending on the resident sites of the doped Fe atom. The findings of the tunable electronic properties and binary magnetic moments of the Fe-doped B_{40}-based metallofullerenes imply that this type of metallofullerene may be applied in single molecular devices.

PACS: 73.61.Wp, 61.72.U−, 81.05.Zx, 81.05.ub DOI: 10.1088/0256-307X/36/11/117302

Inspired by the C_{60}, boron fullerene has attracted especial attention since boron is the nearest neighbor of carbon.[1−5] To date, many boron clusters (B_n) have been reported with n = 3–30, 33–38,..., and so on. Frustratingly, these boron clusters cannot form the fullerene-like structures but possess the geometrical characteristic of the planar, quasi-planar or double-ring tubular-like. In 2008, an eye-catching cage-like B_{80} has been theoretically reported and that immediately intrigued many academic followings about this B_{80}.[1] However, later theoretical computational studies have shown that B_{80} is a high-energy isomer compared with the isomer of core-shell structures.[2] Subsequently, a research also reported the theoretical prediction of a B_{38} cage,[3] while the results are still not of experiment but only from first-principles swarm structure searching calculations. Therefore, over a period of time, whether all-boron fullerene exists or not has remained an open problem. Gratifyingly, this situation was broken by the first discover of the fascinating all-boron fullerene cage-like structure B_{40}, which is uncovered and reported through the combination of the photoelectron spectroscopy and the corresponding theoretical studies.[6] Whereafter, the experimental and theoretical researches jointly confirmed its fullerene hollow cage-like structural characteristic and explicitly proposed the atomic distributed arrangement.[7,8] This fullerene structural characteristic is quite distinguished from the boron clusters of planar, quasi-planar or double-ring tubular-like structures reported previously and thus B_{40} is looked as the second type of single-element fullerene after C_{60}. Therefore, this B_{40} is greatly expected to have extensive and promising applications just like those of carbon fullerene.[9,10] Considering the special hollow cage-like structures, it is natural for this all-boron fullerene as a container to encapsulate the foreign atoms or small molecules. Moreover, the large surface of the fullerene cage is much favorable for the foreign dopant to be adsorbed on. Among all the possible adulterant candidates, transition metal (TM) elements have their own unique prominent advantages and are especially appropriate as dopant due to their commonly appearance during the synthesis of nanomaterials, more dispersive valence electron distributions, as well as much larger covalent radius. For a long time, transition metal based metallofullerenes have been the important study object in the fullerene research field.[11,12] Moreover, motivated by the rise of the spintronics, the magnetic dopant and insertion based on the novel nanostructures have attracted extensive interests for the magnetic applications. Fe is the typical and most common ferromagnetic element. Further investigations into the magnetism and functional properties of Fe atom-dopant newly synthesized B_{40} are thus warranted. In the present work, we perform further study on the functionalized design of the newly synthesized B_{40}, by introducing the Fe atom, to obtain significant novel properties for the applications. This result would be expected to give valuable information for applications of B_{40} on fabricating novel single molecular electronic and spin electronic nanodevices.

All the present calculations are based on the density-functional theory by performing the program SIESTA.[13−15] A flexible linear combination of numerical atomic-orbital basis sets was used for the description of valance electrons, and norm-conserving nonlocal pseudopotentials were adopted for the atomic cores. The generalized gradient approximations (GGA) with the Perdew-Burkle-Ernzerhof (PBE) corrections were adopted and the atomic orbital set employed throughout was a double-ζ plus polarization (DZP) functions. The 3d electron orbitals of the Fe

*Supported by the National Basic Research Program of China under Grant No 2014CB931700, and the State Key Laboratory of Optoelectronic Materials and Technologies.
**Corresponding author. Email: lijiling@mail.sysu.edu.cn
© 2019 Chinese Physical Society and IOP Publishing Ltd

atom were also taken into account. The numerical integrals were performed on a real space grid with an equivalent cutoff of 120 Ry. We use periodic boundary conditions and a supercell large enough to keep a distance of at least 15 Å between neighboring images to avoid the interactions. All the atomic coordinates are relaxed using the conjugate gradient (CG) algorithm, until the maximum atomic forces less than 0.02 eV/Å. To evaluate the stability of the Fe-doped B_{40}-based metallofullerenes, the binding energy (E_b) is calculated by the difference between the total energy of the metallofullerenes and the sum of the total energies of the pristine B_{40} and the isolated Fe atom.

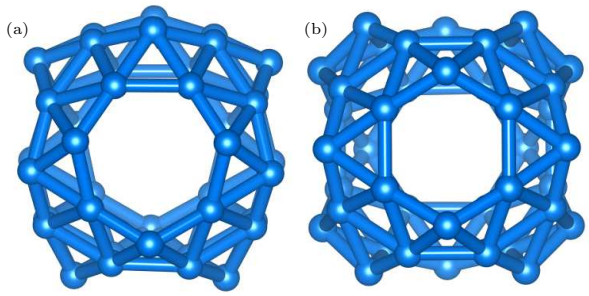


Fig. 1. The optimized configuration of the pristine B_{40}: (a) sideview, and (b) topview.

First, we constructed the exact atomic distribution of B_{40} and performed fully structural optimization. The optimized configuration is shown in Fig. 1. Obviously, the obtained equilibrium configuration exhibits typical fullerene cage-like structural characteristic, with the surface consist of two six-membered rings, four seven-membered rings and several interwoven double boron chains (IDC). The whole fullerene cage shows perfect symmetry of D_{2d} point group. The calculated diameter is 6.36 Å, consistent with that of 6.22Å[6] and slightly smaller than the diameter of 7.10 Å of the C_{60}.[16] According to the symmetrical feature, initially, different representative B_{40}-based metallofullerenes were considered with the doped Fe atom at different sites. After completely structural relaxations, the doped Fe atom obviously tends to reside at different symmetrical sites and correspondingly six stable configurations of the Fe-doped B_{40}-based metallofullerenes were obtained. According to the resident site of the doped Fe atom, the B_{40}-based metallofullerenes are distinguished by designating different names. For the endohedral Fe@B_{40} metallofullerenes, the names of Fe@B_{40}-6R, Fe@B_{40}-7R and Fe@B_{40}-IDC are respectively corresponding to the Fe atom inside the center of six-membered ring, inside the center of seven-membered ring and inside the center of the overlapping of the IDC. Similarly, for the exohedral Fe–B_{40} metallofullerenes, the names of Fe-B_{40}-6R, Fe-B_{40}-7R and Fe-B_{40}-IDC are respectively corresponding to the Fe atom outside the center of six-membered ring, outside the center of seven-membered ring and outside the center of the overlapping of the IDC. All the stable equilibrium configurations are shown in Figs. 2(a)–2(f). To evaluate the stability, the binding energies of the considered Fe-doped metallofullerenes are calculated according to the definition mentioned above. The results are listed in Table 1. Herein, the positive values indicate that the hybridization process for the Fe atom to dope B_{40} is exothermic. As listed in Table 1, the larger binding energies ranging from 3.07 to 5.31 eV/atom indicate that the Fe atom can either be chemically encapsulated inside the cage or adsorbed on the surface of B_{40} and form stable Fe-doped metallofullerenes. Among them, the binding energy of the Fe-B_{40}-IDC metallofullerene is about 1 eV/atom lower than those of other isomers of the Fe-doped metallofullerenes and thus has less stability. However, it is noteworthy that the binding energy of the Fe-B_{40}-IDC metallofullerene is positive and of the value of 3.07 eV/atom. This illustrates that the process of the Fe atom adsorbed outside the center of the overlapping of the IDC is exothermic and the value of 3.07 eV/atom ensures that the corresponding reaction process is chemically adsorbed. Therefore, in spite of the relatively lower binding energy, the Fe-B_{40}-IDC metallofullerene is deduced to be in a metastable state. At present, a number of theoretical and experimental studies have been carried out about the synthesis and properties of the nanomaterials with metastable state. Commonly, the novel nanostructure in metastable states could be synthesized using special methods. For example, the pulsed-laser induced liquid-solid interface reaction (PLIIR) is a specialized method having unique advantage to synthesize the metastable nanomaterials. Therefore, for the energetically favored isomers, it is certainly stability and much easily to be obtained in experiment, while for the metastable Fe-doped metallofullerenes such as the Fe-B_{40}-IDC, we think that the experimental researchers can adopt special experimental methods to synthesize the novel nanostructure.

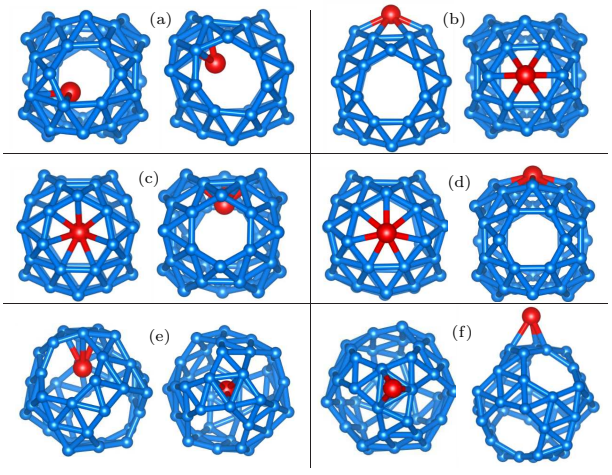


Fig. 2. The sideview and topview of the optimized configurations of the Fe-doped B_{40}-based metallofullerenes: (a) for the Fe@B_{40}-6R, (b) for the Fe-B_{40}-6R, (c) for the Fe@B_{40}-7R, (d) for the Fe-B_{40}-7R, (e) for the Fe@B_{40}-IDC, and (f) for the Fe-B_{40}-IDC. The blue for B and the red for Fe.

To gain additional insights into the interactions of the Fe atom with the fullerene B_{40}, we performed the

calculations of the scan of potential energy by moving the Fe atom from the outside into the inner along with the path crossing the center of six-membered and seven-membered ring respectively by keeping the B_{40} cage intact. The results indicate that there are energy barriers during the approaching process of the Fe atom to B_{40}, which is consistent in the situations previously reported. For example, in the previous work, the energy barriers for the Na atom are about 10 eV for its moving IN and OUT through the heptagon-ring, respectively.[17] Due to the existence of the energy barriers, the metallofullerenes cannot spontaneously adsorb the foreign doped atom into the inner of the cage. However, this does not mean that the synthesis of endohedral metallofullerenes is impossible. Actually, in the past years, the explorations to synthesize the endohedral metallofullerene have been performed extensively and considerable progress has been achieved. In view of the previous numerous reports on endohedral carbon fullerenes, the formation of endohedral metallofullerene, for example, endohedral metallofullerene La@C_{60} was immediately synthesized after the discovery of C_{60} fullerenes. Subsequently, various endohedral metallofullerenes were reported experimentally having different atoms or clusters inside the cage. To date, there are many synthesized methods for the preparation of endohedral metallofullerenes such as DC-arc discharging methods, and chemical vapor deposition. The different dopant types are important for the chemical reaction process and thus determine the corresponding synthetic methods of endohedral metallofullerenes. Furthermore, unlike the C_{60} molecule, B_{40} has larger entrances to the inner: four seven-membered rings and two six-membered rings. The presence of such large holes raised expectations that the penetration of B_{40} by small guest atoms and molecules should be easier than in the case of the carbon fullerenes. Therefore, based on the above discussions, although the energy barriers exist when the Fe atom approaching into B_{40}, the endohedral Fe@B_{40} metallofullerenes could be possibly synthesized.

Table 1. The binding energies of the Fe atom hybridized with B_{40}, the bond length of the formed Fe–B and the elongation of the B–B bonds near the doped sites.

Fe-position	E_b (eV)	Fe–B (Å)	Elongation of B–B (%)
Fe@B_{40}-6R	4.55	2.35	1.52
Fe@B_{40}-7R	4.31	2.25	0.40
Fe@B_{40}-IDC	4.54	2.34	1.11
Fe-B_{40}-6R	4.39	2.06	3.22
Fe-B_{40}-7R	5.31	2.06	2.50
Fe-B_{40}-IDC	3.07	2.44	2.05

We analyze the structural parameters of the equilibrium geometry of each metallofullerene. For the Fe@B_{40}-6R metallofullerene, the encapsulated-Fe atom connects with the B atom by forming the Fe–B bonds of the average length of 2.35 Å. In accompanying, the B–B bonds near the B atoms connecting with Fe atom are elongated, with the average bond length from 1.71 Å to 1.73 Å and the elongation of 1.52%. The corresponding values for other Fe-doped B_{40}-based metallofullerenes can be seen in Table 1. Obviously, for all the metallofullerenes, local structural deformations occur due to the formation of the Fe–B bonds, as can be seen from Figs. 2(a) and 2(f). The explicit hybridization between the doped Fe atom and boron cage and the consequent structural deformations will apparently modulate the electronic interactions, and thus tune the corresponding electronic and the magnetic properties, as discussed in the following.

We then performed the calculations of the electronic properties of all the considered Fe-doped B_{40}-based metallofullerenes. The calculated energy gaps of the highest occupied molecular orbital (HOMO) and the lowest unoccupied molecular orbital (LUMO) are listed in Table 2. Obviously, when the all-boron fullerene B_{40} is doped by the Fe atom, the dopant states are introduced in the energy gap and thus the energy gaps of the metallofullerenes are adjusted and reduced in comparison with 1.72 eV of the pure B_{40}, no matter whether the Fe atom encapsulated in or adsorbed outside the cage. Although the energy gaps based on density functional theory are always underestimated, the change of energy gaps is relative and obtained from the same theoretical levels and thus still significant. Consequently, the electronic properties of the Fe-doped B_{40}-based metallofullerenes can be tailored by changing the position of the doped Fe atom, which is significant for application.

Table 2. The energy gaps E_{gap} of Fe-doped B_{40}-based metallofullerenes, the total magnetic moment M and its contribution from $4s$ (m_{4s}), $3d$ (m_{3d}), and $4p$ (m_{4p}) orbitals.

Fe-position	E_{gap}	M (μ_B)	m_{4s} (μ_B)	m_{3d} (μ_B)	m_{4p} (μ_B)
Fe@B_{40}-6R	1.56	2.00	0.031	2.651	0.108
Fe@B_{40}-7R	1.43	2.00	0.029	2.755	0.073
Fe@B_{40}-IDC	1.60	2.00	0.031	2.629	0.110
Fe-B_{40}-6R	1.31	2.00	0.037	2.256	0.230
Fe-B_{40}-7R	1.50	2.00	0.074	2.194	0.093
Fe-B_{40}-IDC	1.11	4.00	0.451	3.264	0.280

Fe is a typical magnetic element of TM. The magnetic properties of the Fe-doped metallofullerenes are crucial to reveal the nature of the foreign Fe atom hybridization process with the B_{40} cage. The calculated magnetic moments of the Fe-doped metallofullerenes are listed in Table 2. It is obvious that when the doped Fe atom resides inside B_{40}, the calculated total magnetic moments of each Fe@B_{40}-based metallofullerene are $2.00\mu_B$, reduced just half compared with that of $4.00\mu_B$ of the isolated Fe atom. However, for the Fe–B_{40}-based metallofullerenes, the total magnetic moments obtained are divided into two types: (1) when the Fe atom is located outside the center of multiple-membered rings, whether six-membered or seven-membered rings, the total magnetic moments of the corresponding metallofullerenes are $2.00\mu_B$, the same as those of the endohedral Fe-doped metallofullerenes, and (2) when the Fe atom is located outside the center of the overlapping of the IDC, the total magnetic moments of corresponding metallofullerenes

are $4.00\mu_B$, just the same as that of the isolated Fe atom. Therefore, the total magnetic moments of all the Fe-doped B_{40}-based metallofullerenes are alternative between $4.00\mu_B$ and $2.00\mu_B$, indicating binary characteristic. Considering the structural characteristic of B_{40}, Fig. 3 gives the theoretical sketch map of how to selectively obtain the desired total magnetic moments of the metallofullerenes. In Fig. 3(a), when the Fe atom approaches to the boron cage along the direction towards the center of the multiple-membered rings, it will ultimately resides outside the center of the multiple-membered ring or enter into the cage. However, whether it is located outside or inside the cage, the total magnetic moments of the corresponding metallofullerenes are $2.00\mu_B$. On the other hand, when the Fe atom approaches along the direction towards the center of the overlapping of the IDC, it cannot enter into the boron cage and thus ultimately the Fe-B_{40}-IDC metallofullerene is formed with the total magnetic moment of $4.00\mu_B$. Thus it is feasible to control the total magnetic moments of the Fe-doped metallofullerenes by controlling the ways along which the Fe atom approaches to the B_{40} cage. The characteristics of controllable alternative binary magnetic moments are noticeable for the experimental researchers to find a path of synthesis of these promising metallofullerenes.

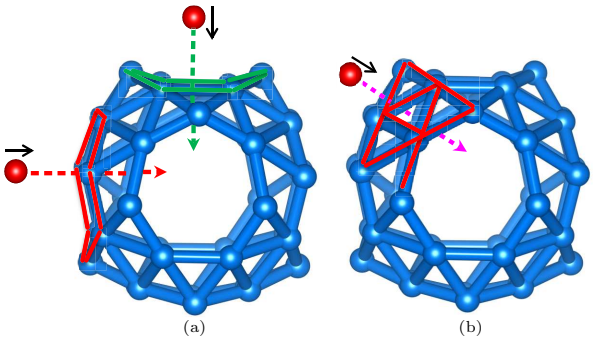


Fig. 3. A sketch map of the ways for the Fe atom approaching and entering into B_{40}: (a) along the way towards the center of the multiple-membered rings, the green and red respectively indicating towards the six-membered ring and seven-membered ring, and (b) the way towards the center of the overlapping of the IDC.

Table 3. Mulliken population analysis of the isolated Fe atom and the Fe atom in the Fe-doped B_{40}-based metallofullerenes. The last column is the quantity of the electron transfer from Fe to B in B_{40}.

Fe-position	Total	Spin up(↑)			Spin down(↓)			Charge transfer $\|e\|$/Fe to B
		4*s*	3*d*	4*p*	4*s*	3*d*	4*p*	
Isolated Fe atom	4.00	1.000	5.000		1.000	1.000		
Fe@B_{40}-6R	2.79	0.219	4.479	0.371	0.188	1.828	0.263	0.652
Fe@B_{40}-7R	2.86	0.225	4.523	0.358	0.196	1.768	0.285	0.647
Fe@B_{40}-IDC	2.77	0.218	4.470	0.369	0.187	1.841	0.259	0.658
Fe-B_{40}-6R	2.53	0.378	4.306	0.493	0.341	2.050	0.263	0.169
Fe-B_{40}-7R	2.36	0.416	4.232	0.449	0.342	2.038	0.356	0.167
Fe-B_{40}-IDC	3.71	0.713	4.712	0.426	0.280	1.448	0.146	0.544

To lend further understanding of the distinctly alternative binary magnetic property, we performed the Mulliken population calculations for the isolated Fe atom and the Fe atom in the metallofullerenes, as listed in Table 3. From the total electron transfer from the Fe atom to B atoms given in the last column in Table 3, the encapsulated Fe atom will introduce more electrons transferring, as the quantities of the transferred electrons ($0.652e$, $0.647e$ and $0.658e$ respectively) are all more than those of the exohedrally adsorbed Fe ($0.169e$, $0.167e$ and $0.544e$, respectively). Accompanying with the electron transfer from the Fe atom to B atoms, the residual electrons in the doped Fe will re-distribute due to the confinement effect of electronic orbitals, including spin-up and spin-down. For the Fe-B_{40}-IDC complex, during the redistribution of the residual electrons, less electrons transfer from 4*s* and 3*d* spin-up orbitals and simultaneously less electrons can be obtained for the 3*d* and 4*p* spin-down orbitals, which leads to minor compensation of spin-up and spin-down and thus larger residual magnetic moments. However, for the Fe-B_{40}-6R and Fe-B_{40}-7R complexes, during the re-distribution of the residual electrons, more electrons transfer from 4*s* and 3*d* spin-up orbitals but simultaneously more electrons can be obtained for the 3*d* and 4*p* spin-down orbitals. As a result, the major compensation of spin-up and spin-down ultimately leads to smaller residual magnetic moments. Therefore, the reason of the difference between the total magnetic moments of the Fe-doped mellofullerenes is just the electron transfer and the resulting redistribution of the electrons between different electronic orbitals due to the confinement effect. The results of the magnetic properties can also be seen from the spin polarized projected density of states (PDOS), as shown in Fig. 4. Wherein, the inset in Fig. 4(a) is the PDOS of the pure B_{40}. As seen in Fig. 4, the majority (spin up) state and minority (spin down) state are partly spin-compensated, resulting in different residues of net spin-states. Specially, for the Fe-B_{40}-IDC metallofullerenes, the net spin-states near the Fermi level introduced in the boron cage are the majority (spin up) states, quite different from the minority (spin down) states of the boron in other metallofullerenes. This is consistent with the calculated total magnetic moments and the alternative binary magnetic properties discussed above. The binary characteristic of the magnetic properties in the Fe-doped B_{40} metallofullerenes are quite different from the TM-doped B-N fullerene-like cage and the

C fullerenes.[18–20] This indicates that the all-boron fullerene B_{40} may have promising applications as single molecular spin devices.

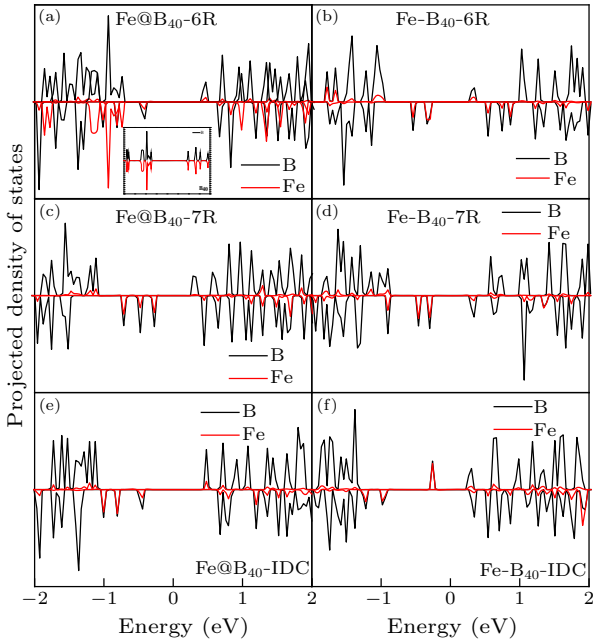


Fig. 4. The spin polarized projected density of states (PDOS) of the Fe-doped B_{40}-based metallofullerenes: (a) for the Fe@B_{40}-6R, (b) for the Fe-B_{40}-6R, (c) for the Fe@B_{40}-7R, (d) for the Fe-B_{40}-7R, (e) for the Fe@B_{40}-IDC, and (f) for the Fe-B_{40}-IDC. The inset is the PDOS of the pure B_{40} and the Fermi levels are all set to zero.

In summary, the stability, electronic and magnetic properties of the Fe-doped B_{40}-based metallofullerenes have been systematically studied. The results indicate that the Fe atom can either be chemically adsorbed on the surface or encapsulated inside B_{40}. Accompanied with the local distortions, the energy gaps can be tailored with different doped sites of the Fe atom. The calculated magnetic moments of the different Fe-doped metallofullerenes are binary, with alternative values between $4.00\mu_B$ and $2.00\mu_B$. The findings of tunable electronic property and the binary magnetic moment of the Fe-doped metallofullerenes proposed here imply B_{40} fullerene, which may be used to develop novel single molecular electronic devices, especially single molecular spin magnetic devices. We hope that the present work can motivate further experimental research on the functionalized methods for the applications of the newly synthesized B_{40}.

References

[1] Szwacki N G, Sadrzadeh A and Yakobson B I 2007 *Phys. Rev. Lett.* **98** 166804
[2] Zhao J J et al 2010 *J. Phys. Chem. A* **114** 9969
[3] Lv J et al 2014 *Nanoscale* **6** 11692
[4] Prasad D L V K and Jemmis E D 2008 *Phys. Rev. Lett.* **100** 165504
[5] Rajendra R Z, Tunna B et al 2009 *Phys. Rev. B* **79** 161403 (R)
[6] Zhai H J, Zhao Y F et al 2014 *Nat. Chem.* **6** 727
[7] Chen Q, Li W L et al 2015 *ACS Nano* **9** 754
[8] He R X and Zeng X C 2015 *Chem. Commun.* **51** 3185
[9] Wei L et al 2015 *Chin. Phys. Lett.* **32** 076501
[10] Li X D, Tang Y J et al 2011 *Chin. Phys. Lett.* **28** 113102
[11] Zhang M, Feng X J et al 2012 *Chin. Phys. B* **21** 056102
[12] Tang C M, Zhu W H et al 2010 *Chin. Phys. B* **19** 033604
[13] Ordejón P, Artacho E and Soler J M 1996 *Phys. Rev. B* **53** R10441
[14] Sánchez-Portal D, Ordejón P, Artacho E and Soler J M 1997 *Int. J. Quantum Chem.* **65** 453
[15] Soler J M et al 2002 *J. Phys.: Condens. Matter* **14** 2745
[16] Kroto H W et al 1985 *Nature* **318** 162
[17] Fa W et al 2015 *J. Phys. Chem. A* **119** 11208
[18] Batista R J C, Mazaoni M S C and Chacham H 2007 *Phys. Rev. B* **75** 035417
[19] Dutty D M and Blackman J A 1998 *Phys. Rev. B* **58** 7443
[20] Yagi Y et al 2004 *Phys. Rev. B* **69** 075414